On the Effects of Blockage on Load Modeling in Millimeter-Wave Cellular Networks

Muhammad Saad Zia, Douglas M. Blough and Mary Ann Weitnauer
School of Electrical and Computer Engineering
Georgia Institute of Technology, Atlanta, Georgia 30332-0250, USA
Email: saad.zia@gatech.edu; doug.blough@ece.gatech.edu; mary.ann.weitnauer@ece.gatech.edu

2021 IEEE 94th Vehicular Technology Conference (VTC2021-Fall) | 978-1-6654-1368-8/21/$31.00 ©2021 IEEE | DOI: 10.1109/VTC2021-FALL52928.2021.9625443

***Abstract*—The sensitivity to blockages at millimeter-wave (mm-wave) frequencies is very different from that at sub-6 GHz frequencies. The blockages affect the user-to-base station (BS) associations and the resulting association regions of the BSs in the network. This in turn alters the load, i.e., the total number of users associated to a BS. In this paper, we use a stochastic blockage model to analyze such effects. We characterize the variation in the load as a function of the blockage environment in a stochastic geometric setting. Our analysis indicates that in the extreme cases of total blocking and no blocking, the mean load on the tagged mm-wave BS is identical to that of a sub-6 GHz BS for a given BS and user density. For intermediate blockage environments, the mean load on the tagged mm-wave BS is found to be less than that on a sub-6 GHz BS. Using Monte-Carlo simulations, we establish that the existing analytical models for load characterization in mm-wave networks result in overestimation of the load per BS and underestimation of the achievable rate.**

***Index Terms*—Load, blockage, LOS probability, Poisson-Voronoi, rate.**

I. Introduction

One of the key techniques to increase the capacity of future cellular systems is the use of millimeter-wave (mm-wave) frequency bands [1]. The recent interest of the academic and industry circles towards the mm-wave frequency bands is driven by the fact that these bands can offer high amounts of unused bandwidth as compared to the currently used sub-6 GHz bands [2].

To harness the potential of mm-wave bands, it is necessary to understand the inherent challenges associated with the propagation of such high frequency waves and to establish the similarities and differences of mm-wave systems with their sub-6 GHz counterparts. Such a comparison entails a thorough and deep understanding of the issues that are specific to the modeling of mm-wave systems from an architectural and mathematical perspective. It also facilitates the system level performance analysis of mm-wave networks. Over the last decade or so, the field of stochastic geometry has been used extensively to model and analyze cellular and ad-hoc networks. It allows to capture the randomness of the network in a tractable form [3].

An important distinction between the mm-wave and sub-6 GHz frequencies is the former's sensitivity to blockages in the propagation environment [4]. Such a characteristic renders the path-loss model to be different than that used for lower frequencies. The effects of blockage on the signal-to-noise ratio (SNR) and signal-to-interference-plus-noise ratio (SINR) of mm-wave systems have been studied in great detail by many authors. However, to the best of our knowledge, no existing work explores how the blockage affects the load distribution for a mm-wave BS. The load represents those users that are served by the same BS. Characterization of the load enables analysis of the achievable rate in the network [5].

In [2], closed-form mathematical expressions were provided for an approximate distribution of the load and its mean value in a Poisson distributed mm-wave cellular network. However, those expressions were adopted from sub-6 GHz networks and depended only the BS and user densities without any explicit consideration of the blockage effects. Also, the same expressions have been adopted in many later works (e.g., [3], [6], [7]) to study different aspects of mm-wave networks.

In this paper, we investigate how a change in the blockage environment alters the load on a mm-wave BS and establish that the existing analytical model fails to capture such an effect. We first describe the details of the existing analytical model for the load. Then, we examine the variations in the load as the blockage environment changes. Based on these variations, we demonstrate that the existing analytical model provides an exaggerated value of the load which results in low data rates.

II. System Model

In this paper, we consider a mm-wave network where the BS locations are modeled in $\mathbb{R}^2$ as a homogeneous Poisson point process (PPP) Φ_B of intensity λ_B. All the BSs transmit at a constant power level P_{d}. Moreover, the users are distributed as an independent homogeneous PPP Φ_u with intensity λ_u. As per the standard practice in stochastic geometric analysis, a *typical user* is assumed to be located at the origin, $\mathcal{O}$. According to Slivnyak's theorem, the addition of this typical user does not disturb the overall statistics of the network [8]. The analysis is performed on the typical user because the performance metrics obtained for it are representative of the overall aggregate network performance [1]. The BS serving the typical user is termed as the *tagged* BS.

The mm-wave propagation is modeled using the two-state statistical link model wherein a link can either be in a line of sight (LOS) state or a non-LOS (NLOS) state [2]. The path-loss for the two states is defined separately [9]. For simplicity of notation, the LOS and NLOS channel states are denoted

as "L" and "N" respectively. We adopt the *floating-intercept* model to quantify the path-loss [10]. If the length of a link is r and the link belongs to the k^{th} channel state for $k \in \{L, N\}$, then the path-loss associated with that link is expressed as

$$L_k(r) = C_k r^{\alpha_k}, \tag{1}$$

where α_k is the slope of the best linear fit to the empirical data and C_k is the corresponding floating intercept.

To model the blockage effects and the statistical link probabilities, we use the generalized LOS ball blockage model [2]. According to this blockage model, the LOS region around a BS/user is characterized by a ball of a specific fixed radius R_B. Within this ball, there is a certain probability, $\mathcal{P}_L$, for a link to be LOS. Outside the ball, every link is considered to be non-LOS (NLOS). The term $\mathcal{P}_L$ is referred to as the *average LOS fractional area* in the network and R_B represents the maximum range of a LOS link. The values of R_B and $\mathcal{P}_L$ depend on the geographic area in which the network is deployed and are obtained empirically. The LOS ball model is an analytical approximation with a relatively simple form, yet it provides SINR statistics that match very well with the SINR obtained in the presence of actual blockages [4]. Fig. 1 shows a snapshot of the network with the ball model.

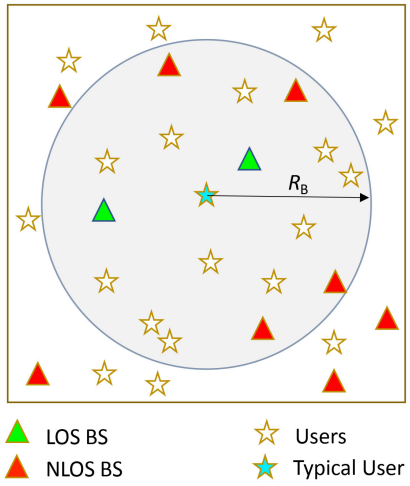

Fig. 1. Generalized LOS ball blockage model from the perspective of the typical user.

The values of different system parameters used in this paper are given in Table I. All these parameters, except λ_B, are adopted from [3].

III. Load Modeling

The load, N, is defined as the number of total users sharing the available time-frequency resources of a BS. In a Poisson distributed network, the load is a random variable (RV) and dictates what fraction of the resources is available to the typical user [5]. The load depends on the user-to-BS association strategy adopted in the network [11]. The association strategy, in turn, specifies the association regions of respective BSs. To analytically characterize the load, the size/area of a BS's association region is required, which itself is a RV. In this paper, each UE is assumed to be served by the BS that offers the maximum average received power (MARP).

TABLE I
Notation and Default System Parameters

Notation	Description	Value
λ_{B}	BS density	$50/\text{km}^2$
λ_{u}	User density	$200/\text{km}^2$
P_{d}	Downlink transmit power	30 dBm
f_{c}	Carrier frequency	28 GHz
W	Bandwidth	1 GHz
$\alpha_{\text{L}}, \alpha_{\text{N}}$	LOS/NLOS path-loss slope respectively	2, 2.92
$C_{\text{L}}, C_{\text{N}}$	LOS/NLOS path-loss intercepts respectively	-61.4 dB, -72 dB
R_{B}	LOS ball radius	200 m

In the following, we first describe how the load is analytically modeled in sub-6 GHz networks and then relate it to a mm-wave network.

A. Sub-6 GHz Networks

In a homogeneous PPP distributed sub-6 GHz network, the MARP-based association becomes the same as the nearest BS association. Such an association scheme gives rise to association regions which form a perfect Poisson-Voronoi tessellation where each user is served by its nearest BS [12]. For Poisson-Voronoi cells, the distribution of the cell area does not exist in a closed-form, however, it can be approximated fairly accurately by a gamma distribution. Using such an approximation, an approximate load distribution was derived in [13] for a homogeneous sub-6 GHz network.

B. Millimeter-Wave Networks

In a network consisting of mm-wave BSs only, the MARP-based association becomes the minimum path-loss based association. Because of the blockage effects and the difference in the path-loss for LOS and NLOS links, the typical user user may connect to a far away LOS BS inside the LOS ball rather than a nearby NLOS BS. This results in an irregular shaped association region for a mm-wave BS, which does not conform to a Poisson-Voronoi cell [2]. It is, therefore, extremely complex to analytically characterize the load in such networks. In [2], however, it was argued that the mean association areas of a mm-wave BS and a perfect Poisson-Voronoi cell are equal and that the approximate load distribution for homogeneous sub-6 GHz networks can also be used to model the load in mm-wave networks. It is important to mention here that the mean value of the area for a Poisson-Voronoi cell is equal to $\frac{1}{\lambda_B}$ [14]. Based on this, the distribution of the total load on the tagged mm-wave BS and its corresponding mean are expressed, respectively, in [2] as

$$\begin{aligned}\mathbb{P}[N=n] = \frac{3.5^{3.5}}{(n-1)!}\frac{\Gamma(n+3.5)}{\Gamma(3.5)}\left(\frac{\lambda_u}{\lambda_B}\right)^{n-1} \\ \times \left(3.5+\frac{\lambda_u}{\lambda_B}\right)^{-(n+3.5)}\end{aligned} \tag{2}$$

$$\mathbb{E}[N] = 1 + 1.28\frac{\lambda_u}{\lambda_B}, \tag{3}$$

where $\Gamma(\cdot)$ is the gamma function.

For a random BS in the network, other than the tagged BS, the load distribution is obtained by multiplying (2) with $\lambda_u/(n\lambda_B)$ and its mean is given by λ_u/λ_B. The use of the above expressions to analytically characterize the load, however, introduces a degree of inaccuracy. This is because the association area of a LOS/NLOS mm-wave BS is approximated by the area of a Poisson-Voronoi cell without considering the effects LOS probability in the network. Note that (2) and (3) depend only on (λ_u/λ_B) and not on $\mathcal{P}_L$. Changing $\mathcal{P}_L$ changes the association probabilities to LOS and NLOS BSs. The LOS ball blockage model further adds to the complexity as it restricts the LOS associations to a certain radius and essentially leads to clipping of the association areas for some of the BSs. In a recent study [14], it was shown that the clipping of a Poisson-Voronoi cell results in the mean area being different from $\frac{1}{\lambda_B}$. Also, with the generalized LOS ball model, Φ_B is sub-divided into two independent non-homogeneous PPPs: a LOS BS PPP and a NLOS BS PPP [1]. Such a distinction, however, is ignored while analytically characterizing the load in (2) and (3).

Based on the above discussion, we argue that the generalized LOS ball blockage model exacerbates the error in the approximation of the analytical load distribution. The distribution in (2) has been used extensively in the literature to model the load in mm-wave networks with the generalized ball model. However, to the best of our knowledge, no existing work explores how the variation in $\mathcal{P}_L$ affects the aforementioned load distribution. To this end, we try to analyze this in the following section.

IV. Effect of LOS Probability on Load Distribution

To study the relationship between the load on a mm-wave BS and the LOS probability of the ball model, we compare the distribution of the load in (2) with the empirical distribution obtained from simulations. For this, $\mathcal{R}_B$ is kept fixed at 200 meters and $\mathcal{P}_L$ is varied from 0 to 1 with a step size of 0.1. The choice of $\mathcal{R}_B = 200$ m is motivated by [2], [3], [6]. The Kullback-Leibler divergence (KLD) [15] is used to quantify the difference between the simulated load distribution, represented as Q_s, and the analytical distribution Q_a, in (2) as

$$KLD\left(Q_s||Q_a\right) = \sum_{n\in\mathcal{Q}} Q_s\left(n\right)\log_2\left(\frac{Q_s\left(n\right)}{Q_a\left(n\right)}\right), \qquad (4)$$

where $\mathcal{Q}$ is the probability space in which both the distributions lie. It is important to note that the KLD compares the two probability distributions over the entire probability space. A higher value of KLD means a greater difference between the analytical and empirical distributions.

For $\lambda_B = 50/\text{km}^2$ and $\lambda_u = 200/\text{km}^2$, the KLD is plotted against different values of $\mathcal{P}_L$ in Fig. 2 for the tagged BS and in Fig. 3 for a BS chosen at random in the network in an area that doesn't include the edge cells. For each value of $\mathcal{P}_L$, 40000 Monte-Carlo trials have been conducted.

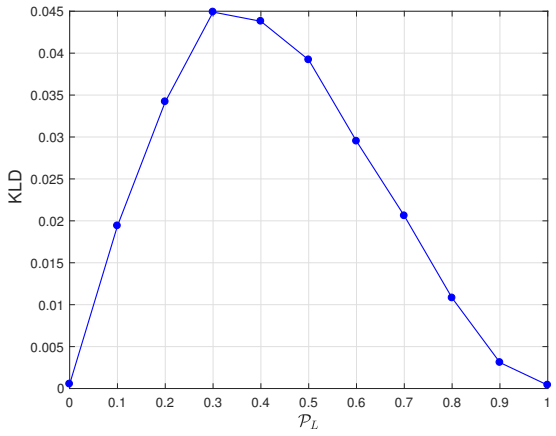

Fig. 2. KLD of the load at the tagged BS as a function of LOS probability

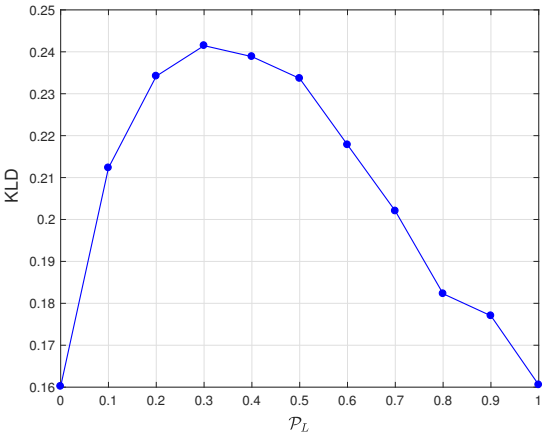

Fig. 3. KLD of the load at a random BS as a function of LOS probability

It is observed that the divergence of the analytical load distribution from the simulated distribution follows the same trend for the tagged BS and any randomly chosen BS. When the LOS probability inside the ball is 0, the network is essentially a homogeneous network since all the BSs are NLOS to all the users (i.e., the LOS ball blockage model does not have any effect) and the divergence between the analytical and empirical distributions in minimum. However, if the value of $\mathcal{P}_L$ is increased from 0, then the divergence also starts to increase as the network no longer remains a homogeneous network. Moreover, the difference between the simulated and analytical load distributions is the greatest at around $\mathcal{P}_L = 0.3$ for the densities under consideration. As the value of $\mathcal{P}_L$ is further increased from 0.3, the irregularly shaped association areas of the mm-wave BSs start to take on some regular shapes ultimately becoming almost identical to Poisson-Voronoi cells at $\mathcal{P}_L = 1$. This discussion based on the KLD establishes that the load on a mm-wave BS varies with changing LOS probability.

To further explore the relationship between the LOS probability and the load, we analyze how the mean load on the tagged BS varies by changing $\mathcal{P}_L$. Fig. 4 plots such a dependence.

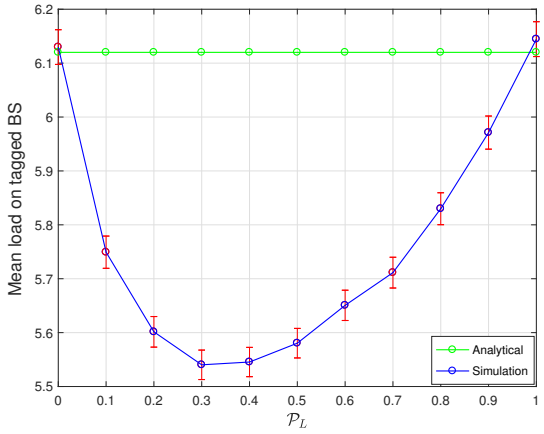

Fig. 4. Variation of the mean load on tagged BS with $\mathcal{P}_L$

The red vertical lines at each value of $\mathcal{P}_L$ in Fig. 4 show the 95% confidence intervals of the mean load obtained from simulations. The relatively small confidence intervals illustrate the accuracy of the trend exhibited by the simulated curve. The green horizontal line shows the analytical mean value of the load obtained from (3), i.e., $\mathbb{E}[N] = 6.12$ for the values of λ_B and λ_u mentioned above. Because the analytical value of mean load is independent of $\mathcal{P}_L$, it remains constant as $\mathcal{P}_L$ varies. It is observed that the simulated mean value of the load is always maximum and almost identical to the analytical mean at $\mathcal{P}_L = 0$ and $\mathcal{P}_L = 1$. For all other values of $\mathcal{P}_L$, the simulated mean load is always less than the analytical mean load. Moreover, the difference between the simulated and analytical mean values of the load is the greatest at around $\mathcal{P}_L = 0.3$ for the densities under consideration. Such a pattern of the difference between the simulated and analytical mean load follows the same trend as the KLD for various values of $\mathcal{P}_L$. From the above results and the corresponding analysis, it can be concluded that for all values of $\mathcal{P}_L$ other than 0 and 1, the approximation in (2) always overestimates the actual load on the tagged mm-wave BS and underestimates the acheivable rate. It is worth mentioning here that while the mean load on the tagged BS changes with $\mathcal{P}_L$, the mean load on a randomly chosen BS in the network remains constant because the users that are dropped by the tagged BS are associated to other BSs in the network.

V. Effect of LOS Probability on Downlink Rate Coverage

The performance of a wireless network is most commonly characterized in terms of the achievable rate. The rate depends on the link quality and the amount of available time-frequency resources. We assume a round-robin scheduling of users where the available resources of a BS are divided equally among the users served by that BS. Using Shannon's capacity formula, the per-user rate in bits per second is expressed as

$$R = \frac{W}{N} \log_2 (1 + \Omega), \tag{5}$$

where W is the total bandwidth available at a BS, N is the total load at the BS and Ω is the SNR or SINR of the desired link. The two RVs in (5), Ω and N, are not independent in general, however, modeling their correlation is highly non-trivial [5]. For the purpose of analytical tractability, therefore, the two aforementioned RVs are assumed to be independent [4]. Because of directional beamforming and the effect of blockages, mm-wave networks are likely to be noise-limited rather than interference-limited with a moderate BS deployment [2]. In [6] and [7], it was verified that with a BS density greater than 50/km^2, the SINR is the same as the SNR. Therefore, in this paper, we assume that our network is noise-limited with $\lambda_B = 50$/km^2 and use the SNR to analyze the rate.

A widely used performance metric to analyze the achievable rate in the network is the rate coverage probability, $\mathcal{R}$, and it represents the probability that the achievable rate at any random user is greater than a certain threshold. It is analogous to the fraction of users in the network which are able to meet predefined thresholds [16]. After some algebraic operations on (5) and utilizing the probability mass function (pmf) of the load given in (2), the rate coverage probability for a given threshold, ρ, is expressed as [4]

$$\mathcal{R}(\rho) = \sum_{n \geq 1} \frac{3.5^{3.5}}{(n-1)!} \frac{\Gamma(n+3.5)}{\Gamma(3.5)} \left(\frac{\lambda_u}{\lambda_B}\right)^{n-1} \times \left(3.5 + \frac{\lambda_u}{\lambda_B}\right)^{-(n+3.5)} C\left(2^{\frac{\rho n}{W}} - 1\right), \tag{6}$$

where $C(\cdot)$ represents the SNR coverage probability. The above expression shows that the rate coverage probability is obtained from the SNR coverage probability, i.e., the CCDF of the SNR distribution [16]. The SNR coverage probability is another metric that is widely used to characterize the performance of stochastic wireless networks and does not depend on the load. A detailed discussion on SNR coverage probability is beyond the scope of this work, therefore, we use the corresponding analytical model and results of [17] to serve our purpose. In [17], the SNR coverage probabilities were obtained for a mm-wave network with perfect and imperfect beam alignment. In this paper, we use only the SNR coverage probability of the perfect beam alignment case considering 32 BS antennas.

The summation in (6) involves infinite terms, but as shown in [4] and [7], fairly accurate results can be obtained by considering a finite maximum number of terms depending on the ratio of user to BS densities. For the densities of Table I, it has been observed that considering the first 24 terms is sufficient.

To corroborate our claim with regards to the underestimation of the rate coverage probability, we study the simulated and analytical rate coverage probabilities for two realistic values of $\mathcal{P}_L$. In the discussion that follows, we compare the difference between the simulated and analytical rate coverage probabilities at a rate threshold value $\rho = 10^9$ for $\mathcal{P}_L = 0.11$ and $\mathcal{P}_L = 0.2$. The reason for choosing these two values of

$\mathcal{P}_L$ is that they have been used most often in the literature for the generalized LOS ball model. In [3], $\mathcal{P}_L = 0.2$ has been used whereas [6] uses $\mathcal{P}_L = 0.11$.

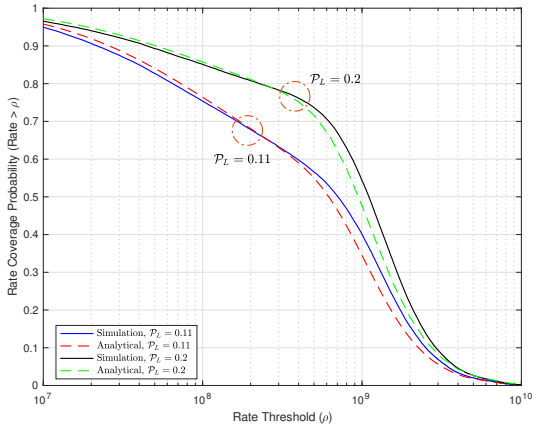

Fig. 5. Simulated and analytical rate coverage probabilities with different values of $\mathcal{P}_L$

Fig. 5 shows the rate coverage probabilities for the above mentioned two values of $\mathcal{P}_L$. The analytical curves match well with the simulations in both the cases. However, a gap starts to appear between them at approximately $\rho = 10^{8.5}$. This value of ρ represents the rates experienced by users at the boundary of the LOS ball. Similar gaps have been observed in existing works on mm-wave networks, e.g. [7], but their relation to the LOS probability has not been explored. The difference between the analytical and simulated rate coverage probabilities becomes quite significant for rate threshold values around 10^9. This region of the curve illustrates the rates experienced by the users that are inside the LOS ball. In this region, the analytical curve is lower as compared to the simulated curve for both the values of $\mathcal{P}_L$. Such an observation further verifies our claim that the analytical load distribution overestimates the load which ultimately results in underestimation of the rate coverage. However, with $\mathcal{P}_L = 0.11$, the analytical curve underestimates the rate coverage probability by 5.43% whereas with $\mathcal{P}_L = 0.2$, it underestimates the rate coverage by 6.64%. As the divergence between the simulated and analytical load distributions is more for $\mathcal{P}_L = 0.2$ as compared to $\mathcal{P}_L = 0.11$, the corresponding difference between the simulated and analytical rate coverage probabilities is also more for $\mathcal{P}_L = 0.2$. The magnitude of these differences in the rate coverage probabilities further validates our earlier observations that changing the value of $\mathcal{P}_L$ alters the distribution of the load on the tagged BS. Such variations in the difference between the simulated and analytical rate coverage probabilities might be insignificant from the perspective of analyzing the achievable rate, but they help in establishing the fact that the LOS probability plays an important role in defining the association areas of the BSs and determining the load served by the tagged BS.

VI. Conclusion

This paper investigates the relation between the blockage in a mm-wave network and the load on a BS. By using the generalized LOS ball model, we show that the load served by the tagged BS varies as the LOS probability inside the ball changes. The already existing analytical model for load characterization, which is based on sub-6 GHz networks, does not model such a relation. Our analysis illustrates that when the LOS probability is either 0 or 1, then the empirical distribution of the load is the same as that provided by the analytical model. However, for other values of the LOS probability, the existing analytical model overestimates the load and underestimates the rate coverage probability in the network.

References

[1] T. Bai and R. W. Heath, "Coverage and rate analysis for millimeter-wave cellular networks," *IEEE Trans. Wireless. Commun.*, vol. 14, no. 2, pp. 1100–1114, Feb. 2015.

[2] S. Singh, M. N. Kulkarni, A. Ghosh, and J. G. Andrews, "Tractable model for rate in self-backhauled millimeter wave cellular networks," *IEEE J. Sel. Areas Commun.*, vol. 33, no. 10, pp. 2196–2211, Oct. 2015.

[3] M. Shi, K. Yang, C. Xing, and R. Fan, "Decoupled heterogeneous networks with millimeter wave small cells," *IEEE Trans. Wireless Commun.*, vol. 17, no. 9, pp. 5871–5884, Sep. 2018.

[4] J. G. Andrews, T. Bai, M. N. Kulkarni, A. Alkhateeb, A. K. Gupta, and R. W. Heath, "Modeling and analyzing millimeter wave cellular systems," *IEEE Trans. Commun.*, vol. 65, no. 1, pp. 403–430, Jan. 2017.

[5] H. S. Dhillon and J. G. Andrews, "Downlink rate distribution in heterogeneous cellular networks under generalized cell selection," *IEEE Wireless Commun. Lett.*, vol. 3, no. 1, pp. 42–45, Feb. 2014.

[6] H. Elshaer, M. N. Kulkarni, F. Boccardi, J. G. Andrews, and M. Dohler, "Downlink and uplink cell association with traditional macrocells and millimeter wave small cells," *IEEE Trans. Wireless Commun.*, vol. 15, no. 9, pp. 6244–6258, Sep. 2016.

[7] M. N. Kulkarni, A. Ghosh, and J. G. Andrews, "A comparison of MIMO techniques in downlink millimeter wave cellular networks with hybrid beamforming," *IEEE Trans. Commun.*, vol. 64, no. 5, pp. 1952–1967, 5 2016.

[8] M. Haenggi, *Stochastic Geometry for Wireless Networks*. Cambridge University Press, 2012.

[9] T. S. Rappaport, G. R. MacCartney, M. K. Samimi, and S. Sun, "Wideband millimeter-wave propagation measurements and channel models for future wireless communication system design," *IEEE Trans. Commun.*, vol. 63, no. 9, pp. 3029–3056, Sep. 2015.

[10] M. R. Akdeniz *et al.*, "Millimeter wave channel modeling and cellular capacity evaluation," *IEEE J. Sel. Areas Commun.*, vol. 32, no. 6, pp. 1164–1179, Jun. 2014.

[11] S. Singh, F. Baccelli, and J. G. Andrews, "On association cells in random heterogeneous networks," *IEEE Wireless Commun. Lett.*, vol. 3, no. 1, pp. 70–73, Feb. 2014.

[12] D. Cao, S. Zhou, and Z. Niu, "Optimal base station density for energy-efficient heterogeneous cellular networks," in *Proc. IEEE Int. Conf. Commun. (ICC)*, 2012, pp. 4379–4383.

[13] S. M. Yu and S.-L. Kim, "Downlink capacity and base station density in cellular networks," in *2013 11th International Symposium and Workshops on Modeling and Optimization in Mobile, Ad Hoc and Wireless Networks (WiOpt)*, 2013, pp. 119–124.

[14] K. Koufos and C. P. Dettmann, "Distribution of cell area in bounded poisson voronoi tessellations with application to secure local connectivity," *J. Statistical Phys.*, vol. 176, no. 5, pp. 1296–1315, 2019.

[15] T. M. Cover and J. A. Thomas, *Elements of Information Theory*. New York, NY, USA: Wiley, 1991.

[16] S. Singh, H. S. Dhillon, and J. G. Andrews, "Offloading in heterogeneous networks: Modeling, analysis, and design insights," *IEEE Trans. Wireless Commun.*, vol. 12, no. 5, pp. 2484–2497, May 2013.

[17] M. S. Zia, D. M. Blough, and M. A. Weitnauer, "Coverage in millimeter-wave networks with SNR-dependent beam alignment errors," in *Proc. IEEE Veh. Technol. Conf. (VTC2020-Spring)*, 2020, pp. 1–5.